An X-Ray Scattering Study into the Structural Basis of Corneal Refractive Function in an Avian Model

Siân R. Morgan,[†] Erin P. Dooley,[†] Paul M. Hocking,[‡] Chris F. Inglehearn,[§] Manir Ali,[§] Thomas L-M. Sorensen,[¶] Keith M. Meek,[†△] and Craig Boote[†△*]

[†]Structural Biophysics Group, School of Optometry and Vision Sciences, Cardiff University, Cardiff, UK; [‡]Roslin Institute and R(D)SVS, University of Edinburgh, Easter Bush, Midlothian, UK; [§]Institute of Molecular Medicine, University of Leeds, Leeds, UK; and [¶]Diamond Light Source Ltd., Didcot, UK

ABSTRACT   Avian vision diseases in which eye growth is compromised are helping to define what governs corneal shape and ultrastructural organization. The highly specific collagen architecture of the main corneal layer, the stroma, is believed to be important for the maintenance of corneal curvature and hence visual quality. Blindness enlarged globe (*beg*) is a recessively inherited condition of chickens characterized by retinal dystrophy and blindness at hatch, with secondary globe enlargement and loss of corneal curvature by 3–4 months. Here we define corneal ultrastructural changes as the *beg* eye develops posthatch, using wide-angle x-ray scattering to map collagen fibril orientation across affected corneas at three posthatch time points. The results disclosed alterations in the bulk alignment of corneal collagen in *beg* chicks compared with age-matched controls. These changes accompanied the eye globe enlargement and corneal flattening observed in affected birds, and were manifested as a progressive loss of circumferential collagen alignment in the peripheral cornea and limbus in birds older than 1 month. Progressive remodeling of peripheral stromal collagen in *beg* birds posthatch may relate to the morphometric changes exhibited by the disease, likely as an extension of myopia-like scleral remodeling triggered by deprivation of a retinal image.

INTRODUCTION

Diseases in poultry that affect normal eye growth and hence impact vision are proving useful for determining what governs the precise size and shape of ocular components (1–6). Compared with other common animal models, such as small mammals and rodents, chicken eyes are more comparable in size to those of humans, and this is beneficial because it facilitates pathological examination and simplifies testing of therapies. Furthermore, the level of conservation between chicken and human genomes is comparable to the degree of genetic homology observed between humans and other mammals that are widely used in medical research (3). These features highlight the potential of chickens as valuable models in the study of human eye diseases.

Conditions characterized by hereditary blindness have been recorded in a number of different strains of chicken (7–13). One such condition is referred to as blindness enlarged globe (*beg*) and is caused by a recessively inherited mutation that arose naturally in Scottish commercial chicken flocks (14). *Beg* mutants have been described as having a complex phenotype that consists of developmental retinal dystrophy and blindness at hatch followed by globe-enlargement and exophthalmus in adult birds (3,14). Pollock et al. (14) reported that at 8 days incubation, small holes are visible in *beg*-affected retinas, which increase in size and result in the developed *beg* chick retina containing many

intracellular spaces. In addition, an abnormal increase in the growth rate of embryonic neural retinal cells was observed during development. Further retinal degeneration occurs in adult birds, with ophthalmic and pathological examinations revealing chorioretinal atrophy, a loss of photoreceptors, and clumping of the retinal pigment epithelium (RPE) (3,14).

Secondary to retinal dysfunction, adult *beg* birds develop markedly larger eye globes and exhibit a reduction in corneal curvature (Fig. 1). The cornea is the major refractive component of the eye in terrestrial vertebrates and is mainly comprised of a complex network of several hundred flattened, interwoven collagen lamellae that form the middle stromal layer and account for >90% of the total corneal thickness (15,16). In the mature chicken cornea there are ~200 stromal lamellae, each having a thickness of 0.25–1.5 μm (17). The precise arrangement of these lamellae is thought to be important for the cornea's ability to endure both physiological and aberrant stresses that can result in debilitating changes in corneal curvature (5,18–20). Indeed, normal corneal curvature is compromised in several conditions affecting both humans and animals that involve pathological modification of stromal architecture (20–23).

Our goal in this study was to undertake the first (to our knowledge) investigation of corneal structure in the *beg* chicken and define any changes in collagen architecture that might help to explain the loss of curvature in these birds. We used wide-angle x-ray scattering (WAXS) to map collagen fibril orientation across the cornea at three posthatch time points, and compared the results with
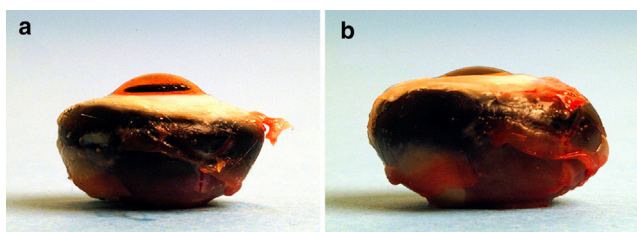
FIGURE 1 Globe enlargement and loss of corneal curvature in *beg*. (*a*) Normal-sighted control eye at 10 months posthatch. (*b*) Age-matched *beg* eye.

equivalent data from previously characterized normal chicken corneas (4,5).

MATERIALS AND METHODS

Animal details

A breeding colony was established and maintained at the Roslin Institute (Edinburgh, UK). The *beg* gene was backcrossed into a line of White Leghorn chickens that are also maintained at Roslin. Chicks were floor-reared with a daily photoperiod of 14 hr of light and 10 hr of darkness, and transferred to individual cages at 16 weeks for single sire-dam matings. All husbandry and experimental techniques were performed under a Home Office project license in accordance with the ARVO statement for the Use of Animals in Ophthalmic and Vision Research. Because the chicks are blind at hatch, they were given extra help by animal-care workers to locate feed and water in the first week of life.

Tissue preparation

Homozygous (*beg/beg*) *beg* chickens were euthanized with an overdose of sodium pentobarbitone at 1, 3, and 9 months posthatch. Immediately after death, the eyes were enucleated and the dorsal position of each cornea was identified with a scleral suture. The eyes were then snap-frozen in liquid nitrogen, transported to Cardiff University on dry ice, and stored at $-80°C$ before experiments were conducted. Immediately before x-ray exposure, nine eyes (each from a different bird, three of each age group) were thawed and the corneas excised, such that 2–3 mm of surrounding scleral tissue was retained.

Clinical and morphometric observations

As reported elsewhere (3,14), homozygous *beg* chickens are blind at hatch but have the same eye weights as normal birds. However, by age 3–4 months, the birds show obvious globe enlargement. As shown in Table 1, a comparison of measurements of axial length (at 6–9 months) in the *beg* birds with age-matched, normal-sighted White and Brown Leghorn chickens were consistent with these previous findings. Physical examination of the enucleated globes revealed noticeable corneal flattening at 9 months, to the extent that the curvature of the cornea was essentially continuous with that of the sclera. In contrast, no visible reduction in curvature was evident at the 1 and 3 month time points.

Data collection

WAXS data were collected at the Diamond Light Source national synchrotron facility (Didcot, UK) on Beamline I02 using a 200 μm × 200 μm x-ray beam of wavelength 0.9796 Å directed perpendicular to the corneal apex. This beam size enabled us to sample an adequate volume of tissue to

TABLE 1 Axial length, IOP, and corneal diameter of blind (*beg/beg*) and sighted control (*beg/+*) chickens

Trait	Age	Vision	Mean	SD	Number
Axial length (mm)	6–9 months	blind	20.73	3.24	12
		sighted	16.86	3.36	11
IOP (mm Hg)	6–9 months	blind	13.81	5.32	8
		sighted	13.77	2.71	11
Corneal diameter (mm)	6–9 months	blind	8.30	0.42	10
		sighted	8.75	0.70	12

Axial length and IOP were determined using a BVI Axis II A-scanner and a Tono-Pen XL (TM) tonometer, respectively, as previously described by Inglehearn et al. (1). The sample sizes differ because the data were generated from different batches of birds. However, all batches were derived at the Roslin Institute from the same bird lines using the same husbandry and maintenance protocols.

generate an acceptable WAXS signal/noise ratio, while minimizing the specimen exposure time to limit radiation damage. To minimize tissue dehydration during x-ray exposure, corneas were wrapped in cling-film and positioned in airtight Perspex (Databank, UK) chambers with Mylar (Dupont-Teijin, UK) windows. We performed raster scans of the entire surface of each cornea at 0.5 mm intervals using motorized specimen translation stages, and collected the resulting scattering data on a Quantum 4R CCD detector (ADSC, Poway, CA) located 550 mm behind the specimen (Fig. 2). The x-ray exposure time per data point was 5–10 s.

Data analysis

By following previously documented methods (24), we acquired the angular intensity profile for each WAXS pattern. These profiles were used to obtain polar vector plots that indicate the orientation of preferentially aligned collagen at each sampled point in the tissue (24). The interpretation of these plots is described in Fig. 3. The polar vector plots were
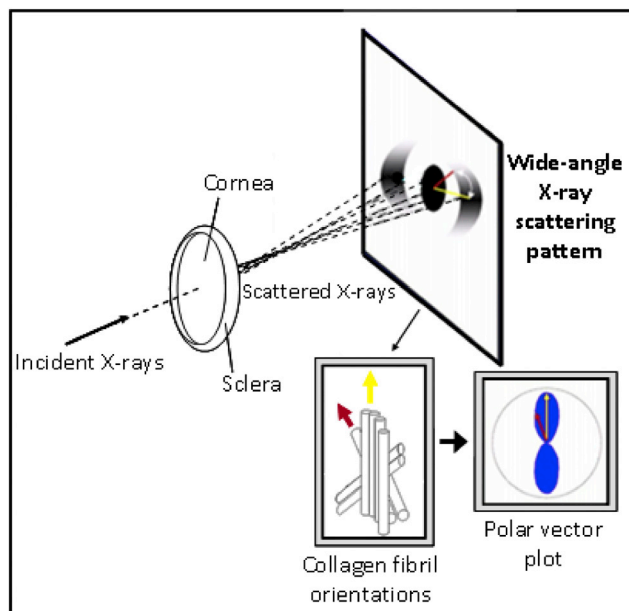

FIGURE 2 X-rays scattered by fibrillar collagen form a scattering pattern on a detector behind the specimen. The WAXS angular intensity profile yields information on collagen orientation. The length of a particular vector in the resulting polar plot is indicative of the number of fibrils preferentially aligned in the vector direction.
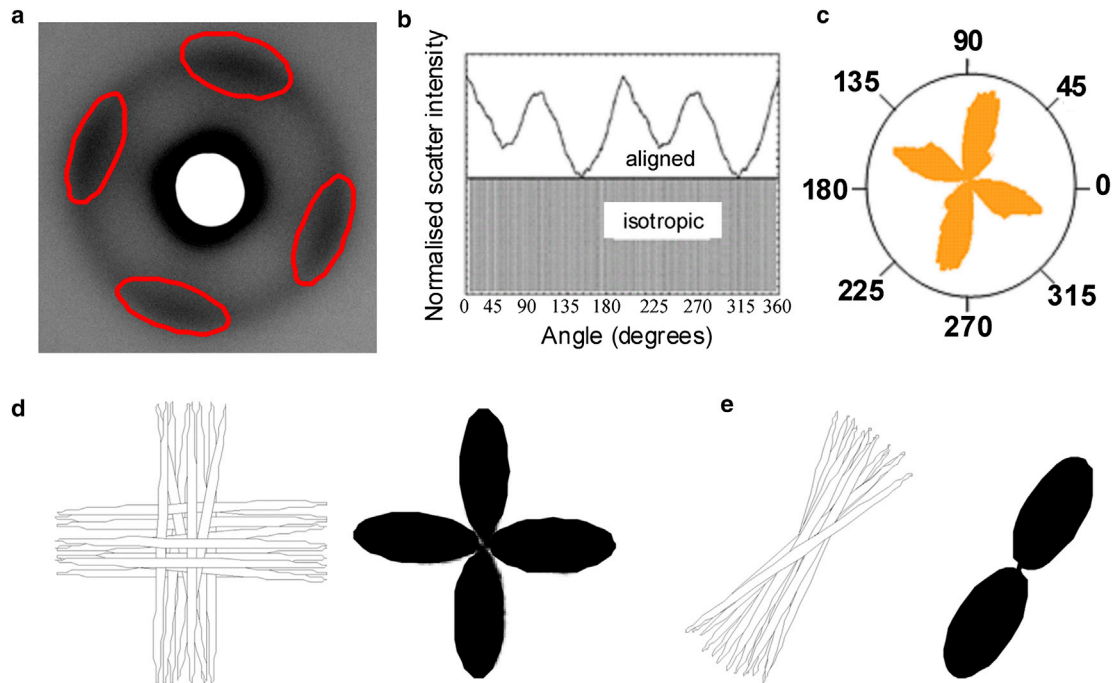
FIGURE 3 (*a*) A typical WAXS pattern from the central normal chick cornea. Uniformly thin, regularly spaced collagen fibrils arranged in all directions within the corneal plane produce a well-defined circular pattern. Lobes of increased intensity arising from x-ray signal perpendicular to the alignment of fibrils are indicated. (*b*) The intensity as a function of angle is measured. (*c*) Scatter from preferentially aligned fibrils is converted into polar vector plots. The radial extent of the resulting plot in a particular direction represents the relative number of collagen fibrils preferentially aligned in that direction. (*d* and *e*) Lamellae are preferentially aligned in an orthogonal and uniaxial orientation, respectively, and the polar vector plots that would represent each arrangement are shown.

compiled and arranged onto a grid according to their geometric positions in the cornea, giving a directional polar vector plot map of the collagen across each specimen. Contour maps, displaying the proportion of collagen at each sampled point that was preferentially aligned, were also produced for the 9-month-old *beg* specimens, as described previously (24). The x-ray scattering technique utilized in this study was previously applied to gather ultrastructural data on wild-type White Leghorn and Isa Brown birds, also bred and maintained at Roslin, at the same posthatch time points used herein (4,5). These age-matched control corneas (three corneas from three birds at each time point) were used for comparison of collagen alignment and distribution in this study. The sampling interval used for the control specimens was 0.4 mm.

Correlation analysis of 9-month-old *beg* birds

We performed a correlation analysis on the fibril orientation distribution functions to detect and quantify the regional extent of differences in collagen alignment in 9-month-old *beg* mutants compared with age-matched controls. This analysis compared the shape of the polar vector plots, and hence the alignment of the collagen, in designated tissue regions, by comparison of the relative x-ray intensity (and hence relative fibril number) at each angle. This method compares only the shape of the plots (relating to the number of fibrils lying along each direction) and ignores the overall size of each plot (related to the overall amount of collagen). Each correlation between corresponding normal and *beg* plots yielded a coefficient value between −1 and +1 that revealed how similar the preferred direction was between them, with a more positive value indicating similarity and a more negative value indicating difference. The center of each cornea was first identified. A central grid of 3×3 patterns, as well as a 3×3 grid in each quadrant of the corneal periphery, was then chosen and the polar plot data within corresponding regions were averaged over the

three corneas for both the *beg* and control groups. For each region, the averaged *beg* data were then correlated against the averaged control using the correlation function shown in Eq. 1, where x_i and y_i represent the corresponding averaged control and *beg* aligned scatter values, respectively, within each angular bin, i. Self-correlations between the three individual 9-month-old *beg* plots and the respective averaged *beg* plots were also performed to determine variability between individual specimens.

$$Correl(X,Y) = \frac{\sum_{i=1}^{256}(x_i - \overline{x}_i)(y_i - \overline{y}_i)}{\sqrt{\left(\sum(x_i - \overline{x}_i)^2 \sum(y_i - \overline{y}_i)^2\right)}} \quad (1)$$

RESULTS

Collagen fibril orientation in the *beg* chicken

The fibril orientation patterns of the aged-matched control corneas used for comparison in this study have been described previously (4,5). In normal birds 1, 3, and 9 months of age, it was shown that the central 2–4 mm of corneal tissue is characterized by a predominantly orthogonal fibril orientation directed along the vertical and horizontal corneal meridians. However, the collagen fibrils toward the corneal periphery adopt, rather abruptly, a preferred tangential orientation, resulting in a pseudoannulus of fibrils that extends into the limbus (4,5). The

pseudoannular arrangement of collagen in the periphery appears more established in older birds, possibly indicating a developmental trend relating to eye growth posthatch (5). At the outer edge of the cornea and in the sclera immediately outside the ossicles, distinct regions of radial fibrillar collagen are also observed, with the corneal population becoming notably less apparent as the birds develop. At 9 months, these are largely absent from the corneal periphery, being replaced mainly by tangential collagen, although the scleral population is still evident (4,5). It was hypothesized that this collagen has a mechanical function related to corneal accommodation, facilitating tension transfer between muscle fibers and the sclera/cornea through association with the ciliary musculature (4), which has insertions in both the sclera, near the ossicles, and in the inner corneal lamellae (25–28). These three discrete structural zones can be seen in Fig. 4, which shows maps of preferential collagen alignment in one control chicken cornea at 1 month posthatch, along with one *beg* chicken cornea of the same age. This figure shows that at 1 month posthatch, no substantial alteration to the preferred collagen orientation is detectable in *beg*-affected corneas. Similar results were obtained for two additional 1-month-old *beg* birds (data not shown).

Collagen orientation at 3 months is displayed in Fig. 5. *Beg* chicken corneas at 3 months posthatch exhibited fibril orientation patterns comparable to those observed in controls in the central (predominantly orthogonal) and outermost regions (radial). The peripheral region of control corneas was not exclusively tangential at this stage, possibly because the eyes were still developing (5). However, in the *beg* corneal periphery, there was more extensive disruption to the fibril pseudoannulus than observed in controls, with more polar vector plots displaying orthogonal (*open triangles*) or near-vertical (*open arrow*) preferential orientation. This pattern of fibril arrangement was also observed in two additional 3-month-old *beg* birds (data not shown).

Fig. 6 shows preferential collagen fibril orientation at 9 months posthatch. As with the control tissue, 9-month-old *beg* corneas were again characterized by a prevalence of orthogonal collagen centrally. However, the disruption that was observed in the peripheral cornea and limbus at 3 months posthatch became much more evident in the 9-month-old *beg* eyes (Fig. 6). Tangentially oriented collagen structures were still present, but the *beg* corneas had a much greater proportion of peripheral fibrils that had adopted an orthogonal (*open triangles*) or near-vertical
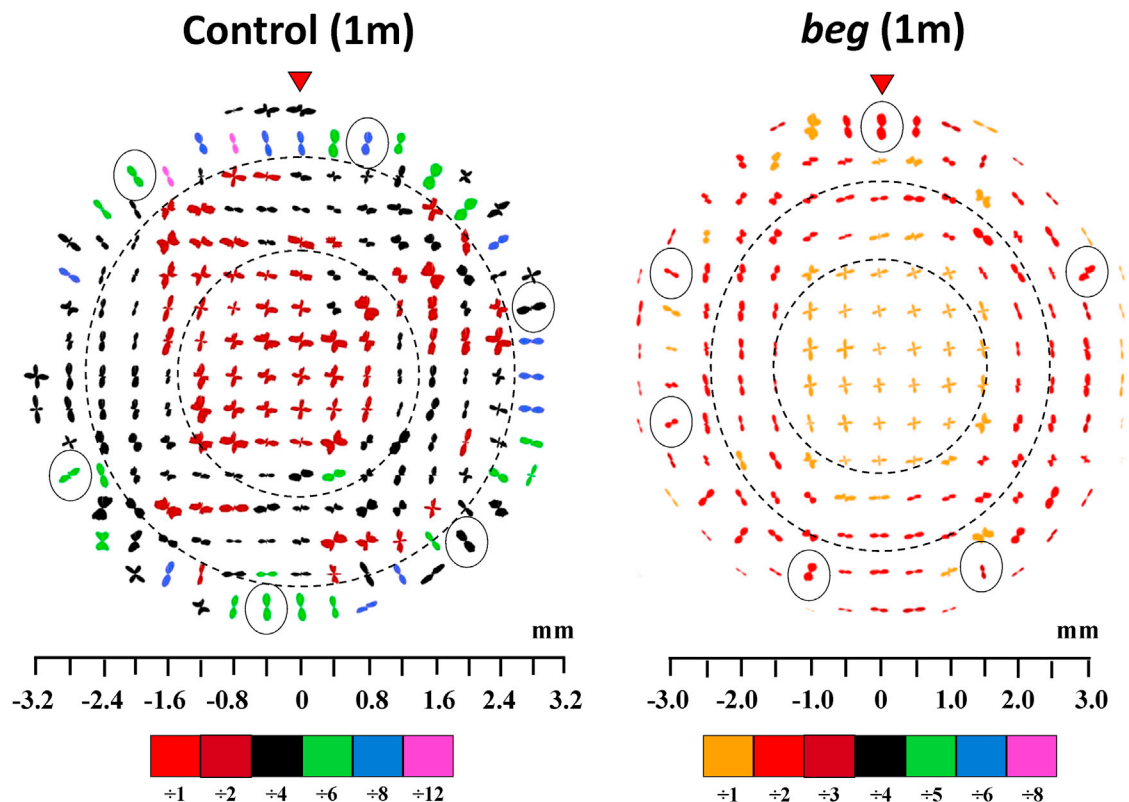

FIGURE 4 Polar vector plot maps showing the preferred orientation of collagen fibrils in the cornea and limbus of one control and one *beg*-affected eye at 1 month posthatch, sampled at 0.4 mm (control) and 0.5 mm (*beg*) intervals. It was necessary to scale down the larger plots for montage display, as indicated in the color keys below each map. Broken lines mark the boundaries of the three structurally distinct regions of the cornea (the central orthogonal region, the peripheral pseudoannulus, and the outermost radial zone). Open circles show radial fibrils in the outermost tissue that may associate with ciliary musculature, and red arrowheads highlight the superior globe position. Control data reproduced from Boote et al. (5).
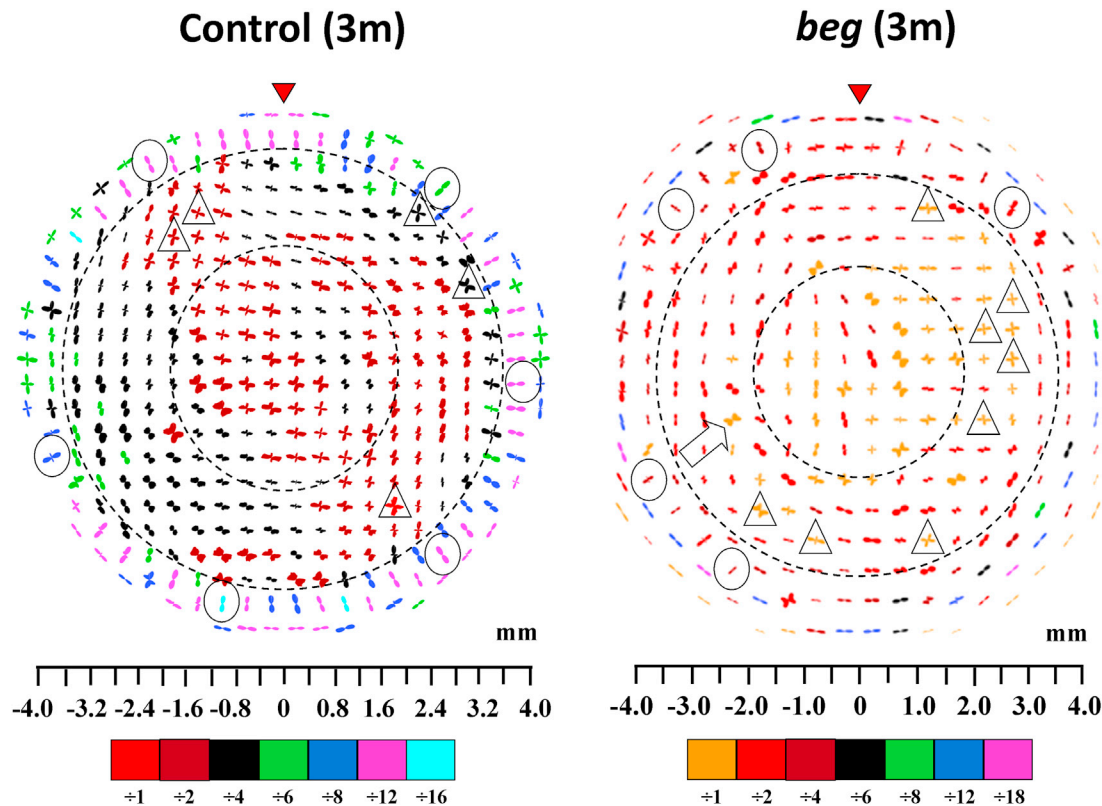
Control (3m)

beg (3m)

FIGURE 5 Preferred orientation of collagen fibrils in the cornea and limbus of one control and one *beg*-affected eye at 3 months posthatch, sampled at 0.4 mm (control) and 0.5 mm (*beg*) intervals. There is more localized disturbance to the collagen pseudoannulus circumscribing the cornea in *beg* birds than in controls, where the normal predominantly tangential fibril alignment is more often replaced by orthogonal (*inside open triangle*) or near-vertical (*open arrows*). It was necessary to scale down the larger plots for montage display, as indicated in the color keys below each map. Broken lines mark the boundaries of the three structurally distinct regions of the cornea (the central orthogonal region, the peripheral pseudoannulus, and the outermost radial zone). Open circles show radial fibrils in the outermost tissue that may associate with ciliary musculature, and red arrowheads highlight the superior globe position. Control data reproduced from Boote et al. (5).

(*open arrows*) preferred orientation than in the normal corneas (Fig. 6), resulting in widespread disruption of the fibril pseudoannulus. We identified this arrangement in all three *beg* birds (data for one bird are shown).

The relative degree of peripheral disruption at 1, 3, and 9 months, as well as the variation between specimens, was further quantified by calculating the percentage of sampling points in the corneal periphery that displayed abnormal (i.e., nontangential) collagen orientation, both individually per specimen and as an average of the three corneas within each time point (Table 2). Reference to this table confirms that peripheral disruption to normal collagen fibrillar arrangement increased significantly over time.

Contour maps showing the spatial variation in the proportion of preferentially aligned collagen across the 9-month-old posthatch control and *beg* corneas are shown in Fig. 7. The central portion of control eyes was found to be relatively uniform; however, in oblique peripheral regions corresponding to the circumferential collagen, there were localized areas of increased alignment (Fig. 7). Notably, although the central portion of the *beg* corneas was found to be similarly uniform compared with controls, the areas

of increased aligned collagen in the corneal periphery and limbus exhibited by the controls were generally weaker and less clearly defined in *beg* (Fig. 7).

Correlation analysis of preferred fibril alignment at 9 months

The similarities and differences in collagen alignment between 9-month-old *beg* corneas and age-matched controls are shown in Fig. 8. The averaged *beg* polar vector plot in the central cornea appeared very similar to the corresponding average control plot, indicating comparable preferred collagen fibril arrangements centrally (Fig. 8 A). This was confirmed by a correlation analysis, in which the central correlation value was strongly positive. Self-correlation further supported this, revealing highly positive correlations between all three individual 9-month-old *beg* corneas in the central region (Fig. 8 B). In contrast, the averaged polar vector plots in the peripheral regions visibly indicated extensive changes in *beg* compared with controls, particularly in the superior quadrants (Fig. 8 A). This is supported by a correlation analysis of the two superior quadrants, which
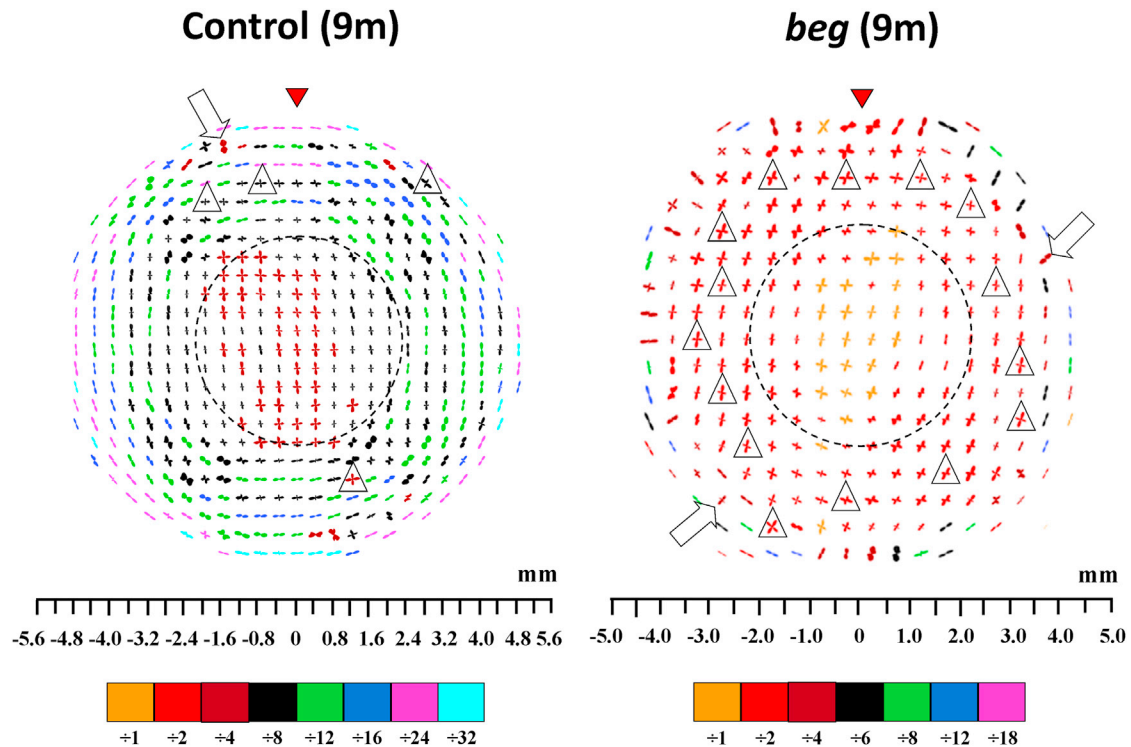
FIGURE 6 Preferred orientation of collagen fibrils in the cornea and limbus of one control and one *beg* chicken at 9 months posthatch, sampled at 0.4 mm (control) and 0.5 mm (*beg*) intervals. There is more severe disturbance to the collagen pseudoannulus at 9 months posthatch than at 3 months. At 9 months, circumferential collagen in the corneal periphery is predominantly orthogonal (*inside open triangles*) or near-vertical (*open arrows*) in orientation. The larger peripheral plots were scaled down for montage display, as indicated in the color keys below each map. Broken lines mark the boundaries of the two structurally distinct regions of the cornea (the central orthogonal region and the peripheral pseudoannular zone). Red arrowheads highlight the superior globe position. Control data reproduced from Boote et al. (4).

produced a negative correlation value when compared with the averaged control plots (Fig. 8 *A*). These corresponded to regions in which the tangential orientation displayed in control eyes was replaced by fibrils with an orthogonal, vertical, or radial preferred orientation. Compared with the superior quadrant, the two inferior quadrants exhibited far more subtle changes overall, consistent with the positive correlation

values obtained for the averaged data (Fig. 8 *A*), and it is clear from the individual *beg* results that this derives from both inferior quadrants retaining significant tangentially oriented collagen, particularly for specimen 861R (Fig. 8 *B*).

DISCUSSION

The relationship between corneal shape and the precise stress-bearing collagenous ultrastructure still needs to be fully elucidated, particularly with regard to changes that occur in pathological tissue. Here we report the posthatch alterations in corneal collagen fibril architecture that accompany loss of corneal curvature and globe enlargement in pathological *beg* chickens. Before we can discuss the potential implications of these results, it is instructive to review collagen architecture in the normal chicken cornea. Previous work has shown that the normal mature chicken corneal stroma can be divided into two structurally distinct regions (4,17). The corneal center, a region of ~2–4 mm, is characterized by a predominance of deep-lying, orthogonally arranged fibrils aligned along the superior-inferior and nasal-temporal meridians. These fibrils, in being directed toward the ocular rectus muscles, may have a stress-bearing function related to eye movement (4). In the peripheral cornea and limbus, the orientation of fibrils alters in favor

TABLE 2 Quantitative comparison of *beg* samples at 1, 3, and 9 months posthatch, and their respective interspecimen variation

Age (bird code)	Percentage of nontangential plots in periphery	Average percentage of nontangential plots in periphery	SD
1 month (1m806R)	14.6	17.2	6.9
1 month (1m839L)	12.1		
1 month (1m857L)	25.0		
3 months (3m836L)	34.7	36.4	4.1
3 months (3m848L)	41.1		
3 months (3m845R)	33.3		
9 months (9m806L)	55.7	58.8	11.9
9 months (9m861R)	48.7		
9 months (9m878L)	71.9		

Percentage of plots in the peripheral pseudoannulus where the normal tangential fibril alignment has been replaced by a preferentially nontangential orientation (orthogonal or near-vertical).
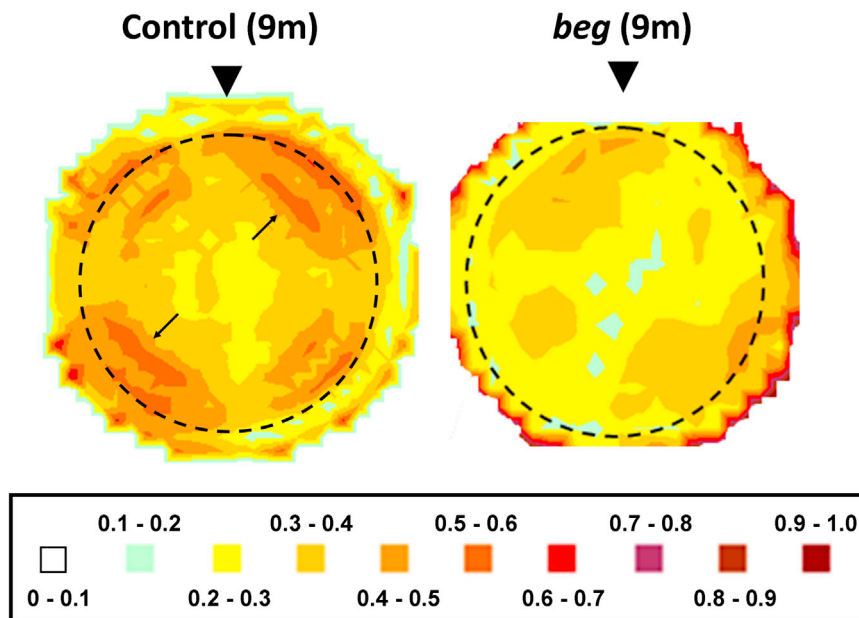
Control (9m)   *beg* (9m)

FIGURE 7 Contour maps showing the spatial variation of the proportion of preferentially aligned collagen across one control and one *beg* chicken cornea at 9 months posthatch. Arrows indicate regions of heightened alignment in the peripheral cornea and limbus of the 9-month-old control eye, suggesting local reinforcement of tangential collagen. These are less pronounced in the bird affected by *beg*. The limbus is marked by a dotted line. Arrowheads highlight the superior globe position. Control data reproduced from Boote et al. (4).

of a predominantly tangential arrangement, locally reinforced in places, forming a pseudoannulus that circumscribes the cornea (4,17). This may be required to take up the increased circumferential limbal stress brought about by the different curvatures of the cornea and sclera (5).

The results presented herein show progressive alterations to peripheral collagen fibril orientations in the *beg* chicken cornea posthatch. These changes were accompanied by globe enlargement and loss of corneal curvature at 9 months. We performed a correlation analysis on the oldest posthatch time point, corresponding to the most severe changes, to quantify the changes in preferential fibril alignment and compare them between designated regions of *beg* and control corneas. This analysis confirmed a loss of the tangentially orientated fibrils that characterize the peripheral cornea and limbus in the normal chicken, in favor of collagen aligned orthogonally, vertically, or radially.

It is our contention that these observations reflect a redistribution of peripheral lamellae in the *beg* cornea, and that these are linked to the corneal flattening presented by the disease. Notably, alterations to peripheral collagen architecture similar to those presented herein have been reported in retinopathy globe enlarged (*rge*) (4,5), an inherited disease of chickens that is also characterized by retinal dysfunction and blindness (1,2,12,13,29). Similarly to *beg* chickens, *rge* birds also exhibit globe enlargement and flattening of the cornea (1,2), changes that have been shown to be compatible with mechanical alteration of the tissue (6) and loss of corneal curvature (5). Although both conditions lead to progressive loss of peripheral tangential collagen, at 9 months the changes observed in *beg* chickens do not appear as extreme as those seen in *rge* chickens (4,5). With this in mind, it is relevant to note that the morphometric changes

are also less severe in the *beg* condition than in *rge*. The increase in axial length and eye weight is markedly smaller in *beg* eyes than in *rge*, suggesting that globe enlargement is less pronounced (Table 3). It may also be significant that *rge* birds become functionally blind at 30–90 days of age (1,2,29), whereas *beg* chicks are blind at hatch (3,14). Despite a marginally greater intraocular pressure (IOP) increase in *rge* eyes, there was no substantial change in either condition, as measured with a Tonopen (Table 3). However, the loss of corneal curvature in birds affected by these conditions could alter the reading obtained with this instrument, so an increase in IOP cannot be dismissed (1). We hypothesize that differences in the extent of globe enlargement between *rge* and *beg*, possibly linked to the timing of vision loss, may be related to the different severity of ultrastructural corneal changes observed in these conditions.

It remains to be established how the corneal alterations observed in *beg* are connected to the retinal deterioration and globe enlargement features of the disease. Our findings indicate that the corneal and globe changes are concomitant between 1 and 3 months posthatch and therefore are likely to be related. This further suggests that these events are elicited by the preceding loss of functional vision that occurs during development (3,14). As with *rge*, the corneal collagen reorganization in *beg* is largely confined to the tissue periphery, implying that the corneal changes may be secondary events to those that are manifest in the sclera (5). During myopia development, an increase in the axial length of the eye is associated with numerous scleral extracellular matrix modifications (30–35). In *beg* birds, it is possible that globe enlargement and loss of corneal curvature are initiated by signals passed from the retina to the sclera through mechanisms similar to those seen in chick
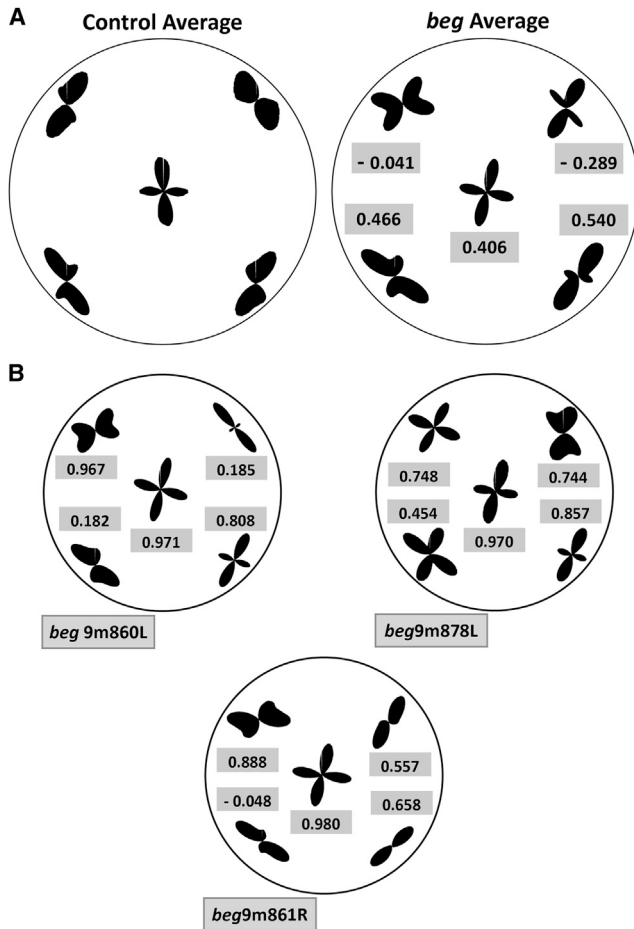
FIGURE 8 Differences in collagen alignment in 9-month-old *beg* mutants compared with age-matched controls. (*A*) Averaged polar vector plots for both 9-month-old control and *beg* chicken corneas, with corresponding correlation values. (*B*) Regional polar vector plots for individual 9-month-old *beg* corneas and corresponding self-correlation values for the averaged *beg* plot.

form-deprivation myopia, where deprivation of the retinal image gives rise to similar morphometric changes (36–38).

In summary, our findings support an association between structural disruption of the collagen network and shape changes in the *beg* cornea. However, this study cannot elucidate whether this structural disruption is a cause or effect of the corneal flattening, and the mechanism that propels these ultrastructural changes remains to be determined. Future characterizations of corneal cellular activity (more specifically modifications to the size, shape, and quantity of keratocytes in the stroma and the volume of collagen they are producing) and/or biochemical analyses of the activity of matrix-degrading enzymes (e.g., metalloproteinases) could reveal whether any active matrix remodeling is taking place in the *beg* cornea. Moreover, we cannot rule out a possible contribution of IOP, because it is difficult to measure this parameter in curvature-affected eyes. Nevertheless, our structural results highlight the *beg* chicken's potential as a valuable animal model for exploring how pathological modification of stromal collagen architecture may affect tissue form and function.

REFERENCES

1. Inglehearn, C. F., D. R. Morrice, …, D. W. Burt. 2003. Genetic, ophthalmic, morphometric and histopathological analysis of the Retinopathy Globe Enlarged (rge) chicken. *Mol. Vis.* 9:295–300.

2. Montiani-Ferreira, F., T. Li, …, S. M. Petersen-Jones. 2003. Clinical features of the retinopathy, globe enlarged (rge) chick phenotype. *Vision Res.* 43:2009–2018.

3. Inglehearn, C. F., M. D. Mohamed, …, P. M. Hocking. 2004. Blindness enlarged globe (beg), a recessively inherited mutation in chickens. *Invest. Ophthalmol. Vis. Sci.* 45:3588.

4. Boote, C., S. Hayes, …, K. M. Meek. 2008. Collagen organization in the chicken cornea and structural alterations in the retinopathy, globe enlarged (rge) phenotype—an X-ray diffraction study. *J. Struct. Biol.* 161:1–8.

5. Boote, C., S. Hayes, …, K. M. Meek. 2009. Ultrastructural changes in the retinopathy, globe enlarged (rge) chick cornea. *J. Struct. Biol.* 166:195–204.

6. Boote, C., A. Elsheikh, …, K. M. Meek. 2011. The influence of lamellar orientation on corneal material behavior: biomechanical and structural changes in an avian corneal disorder. *Invest. Ophthalmol. Vis. Sci.* 52:1243–1251.

7. Hutt, F. B. 1935. Hereditary blindness in the fowl. *Poult. Sci.* 14:297.

8. Randall, C. J., and I. McLachlan. 1979. Retinopathy in commercial layers. *Vet. Rec.* 105:41–42.

9. Cheng, K. M., R. N. Shoffner, …, J. J. Bitgood. 1980. An autosomal recessive blind mutant in the chicken. *Poult. Sci.* 59:2179–2181.

10. Wilson, M. A., B. J. Pollock, …, C. J. Randall. 1982. Early development of a new RP-like mutant in the chick. *In* Problems of Normal and Genetically Abnormal Retinas. R. M. Clayton, H. W. Reading, J. Haywood, and A. Wright., editors. Academic Press, London. 233–239.

11. Wolf, E. D. 1982. An inherited retinal abnormality in Rhode Island red chickens. *In* Problems of Normal and Genetically Abnormal Retinas. R. M. Clayton, H. W. Reading, J. Haywood, and A. Wright, editors. Academic Press, London. 249–252.

TABLE 3 Comparison of the mean increase in axial length and IOP between blind (*beg/beg* and *rge/rge*) and sighted control (*beg/+* and *rge/+*) chickens

Comparison with age-matched sighted controls	Blind (*beg/beg*), 6–9 months	Blind (*rge/rge*), 6–10 months
Increase in axial length (mm)[a]	3.87	6.4
Increase in IOP (mm Hg)[b]	0.04	1.5

The sample sizes differ because the data were generated from different batches of birds. However, all batches were derived at the Roslin Institute from the same bird lines using the same husbandry and maintenance protocols; *rge* data were reproduced from Inglehearn et al. (1).
[a]$n = 10$ (*rge/+*), $n = 11$ (*beg/+*), $n = 12$ (*beg/beg*), $n = 11$ (*rge/rge*).
[b]$n = 10$ (*rge/+*), $n = 11$ (*beg/+*), $n = 8$ (*beg/beg*), $n = 11$ (*rge/rge*).

12. Curtis, P. E., J. R. Baker, …, A. Johnston. 1987. Impaired vision in chickens associated with retinal defects. *Vet. Rec.* 120:113–114.

13. Curtis, R., J. R. Baker, …, A. Johnston. 1988. An inherited retinopathy in commercial breeding chickens. *Avian Pathol.* 17:87–99.

14. Pollock, B. J., M. A. Wilson, …, R. M. Clayton. 1982. Preliminary observations of a new blind chick mutant (beg). *In* Problems of Normal and Genetically Abnormal Retinas. R. M. Clayton, H. W. Reading, J. Haywood, and A. Wright, editors. Academic Press, London. 241–247.

15. Maurice, D. M. 1957. The structure and transparency of the cornea. *J. Physiol.* 136:263–286.

16. Komai, Y., and T. Ushiki. 1991. The three-dimensional organization of collagen fibrils in the human cornea and sclera. *Invest. Ophthalmol. Vis. Sci.* 32:2244–2258.

17. Lucio, A., and R. L. Smith. 1984. Architecture of the corneal stroma of the hen. *Acta Anat. (Basel)* 120:196–201.

18. Maurice, D. M. 1984. The cornea and sclera. *In* The Eye. H. Davson, editor. Academic Press, Orlando 1–158.

19. Boote, C., S. Dennis, …, K. M. Meek. 2005. Lamellar orientation in human cornea in relation to mechanical properties. *J. Struct. Biol.* 149:1–6.

20. Meek, K. M., S. J. Tuft, …, A. J. Bron. 2005. Changes in collagen orientation and distribution in keratoconus corneas. *Invest. Ophthalmol. Vis. Sci.* 46:1948–1956.

21. Daxer, A., and P. Fratzl. 1997. Collagen fibril orientation in the human corneal stroma and its implication in keratoconus. *Invest. Ophthalmol. Vis. Sci.* 38:121–129.

22. Quantock, A. J., S. Dennis, …, M. Tachibana. 2003. Annulus of collagen fibrils in mouse cornea and structural matrix alterations in a murine-specific keratopathy. *Invest. Ophthalmol. Vis. Sci.* 44:1906–1911.

23. Hayes, S., C. Boote, …, K. M. Meek. 2007. A study of corneal thickness, shape and collagen organisation in keratoconus using videokeratography and X-ray scattering techniques. *Exp. Eye Res.* 84:423–434.

24. Meek, K. M., and C. Boote. 2009. The use of X-ray scattering techniques to quantify the orientation and distribution of collagen in the corneal stroma. *Prog. Retin. Eye Res.* 28:369–392.

25. Linsenmayer, T. F., E. Gibney, and J. M. Fitch. 1986. Embryonic avian cornea contains layers of collagen with greater than average stability. *J. Cell Biol.* 103:1587–1593.

26. Glasser, A., D. Troilo, and H. C. Howland. 1994. The mechanism of corneal accommodation in chicks. *Vision Res.* 34:1549–1566.

27. Murphy, C. J., A. Glasser, and H. C. Howland. 1995. The anatomy of the ciliary region of the chicken eye. *Invest. Ophthalmol. Vis. Sci.* 36:889–896.

28. Pardue, M. T., and J. G. Sivak. 1997. The functional anatomy of the ciliary muscle in four avian species. *Brain Behav. Evol.* 49:295–311.

29. Montiani-Ferreira, F., A. Fischer, …, S. M. Petersen-Jones. 2005. Detailed histopathologic characterization of the retinopathy, globe enlarged (rge) chick phenotype. *Mol. Vis.* 11:11–27.

30. Liu, K. R., M. S. Chen, and L. S. Ko. 1986. Electron microscopic studies of the scleral collagen fiber in excessively high myopia. *Taiwan Yi Xue Hui Za Zhi* 85:1032–1038.

31. Funata, M., and T. Tokoro. 1990. Scleral change in experimentally myopic monkeys. *Graefes Arch. Clin. Exp. Ophthalmol.* 228:174–179.

32. Norton, T. T., and J. A. Rada. 1995. Reduced extracellular matrix in mammalian sclera with induced myopia. *Vision Res.* 35:1271–1281.

33. Rada, J. A., D. L. Nickla, and D. Troilo. 2000. Decreased proteoglycan synthesis associated with form deprivation myopia in mature primate eyes. *Invest. Ophthalmol. Vis. Sci.* 41:2050–2058.

34. McBrien, N. A., L. M. Cornell, and A. Gentle. 2001. Structural and ultrastructural changes to the sclera in a mammalian model of high myopia. *Invest. Ophthalmol. Vis. Sci.* 42:2179–2187.

35. McBrien, N. A., and A. Gentle. 2003. Role of the sclera in the development and pathological complications of myopia. *Prog. Retin. Eye Res.* 22:307–338.

36. Gottlieb, M. D., L. A. Fugate-Wentzek, and J. Wallman. 1987. Different visual deprivations produce different ametropias and different eye shapes. *Invest. Ophthalmol. Vis. Sci.* 28:1225–1235.

37. Irving, E. L., J. G. Sivak, and M. G. Callender. 1992. Refractive plasticity of the developing chick eye. *Ophthalmic Physiol. Opt.* 12:448–456.

38. Troilo, D., T. Li, …, H. C. Howland. 1995. Differences in eye growth and the response to visual deprivation in different strains of chicken. *Vision Res.* 35:1211–1216.